



Application of direct-injection detector integrated with the multi-pumping flow system to photometric stop-flow determination of total iron

Stanislawa Koronkiewicz*, Sławomir Kalinowski

University of Warmia and Mazury, Department of Chemistry, 10-957 Olsztyn, Poland

ARTICLE INFO

Article history:

Received 3 November 2011

Received in revised form 27 February 2012

Accepted 2 March 2012

Available online 15 March 2012

Keywords:

Flow analysis

Multi-pumping flow system

Direct-injection detector

Light-emitting diode

Paired emitter-detector diode

ABSTRACT

A novel direct-injection detector (DID) integrated with multi-pumping flow system (MPFS) for the photometric determination of iron is proposed. Paired emitter-detector diodes have been used as a photometric detection system. The sample and reagent were injected using appropriate solenoid pulse micro-pumps directly into the detection chamber where effective mixing occurred. The use of proposed stop-flow detector considerably simplified the analytical procedure. The potassium thiocyanate has been chosen as a chromogenic reagent for photometric Fe(III) detection. The total volume of reagent and sample/standard solutions involved in the detection process was adjusted to the volume of the reaction-detection chamber.

Calibration graph was found to be linear in the range up to 10 mg L^{-1} . The detection limit ($3s_b/S$) was 0.15 mg L^{-1} . The repeatability (R.S.D.), calculated from 10 analyses of sample containing 5 mg L^{-1} Fe(III), was 1.5% and the sample throughput 180 determinations per hour. The consumption of sample and reagent was $20 \mu\text{L}$ each with the waste generation at the level of 0.24 mL . The applicability of the proposed method to the determination of total iron in groundwater samples has been proved.

The analytical parameters are compared to those obtained exploiting the MPFS system with typical configuration containing a confluence point and reaction coil.

© 2012 Elsevier B.V. All rights reserved.

1. Introduction

Flow systems are very common in routine analysis, mainly because they provide high precision and rapid measurements with minimal sample handling. Another advantage is a low consumption of sample and reagents in comparison to the batch methods. The most widely used flow technique is still the flow injection analysis (FIA) [1]. However, a new trend in modern chemical analysis imposes the need to develop fully automated systems. Additionally, from the point of view of Green Chemistry, an even greater reduction in reagent and energy consumption is required.

Multicommutated flow techniques have been growing rapidly for several years. Among them, multi-pumping flow systems (MPFS) seem to be a very interesting alternative to classical flow techniques [2–5]. Multi-pumping flow systems utilizing solenoid pulse micro-pumps acting as the liquid propelling units. Moreover, they are responsible for the sample and reagents introduction and commutation of the flow system [6]. In the MPFS, reagents are propelled into the system only when necessary. No continuous motion of

carrier solution occurs. Therefore, the low reagent consumption and waste generation in this technique is highlighted and the MPFS is regarded as an environmentally friendly alternative to the FIA [7]. The replacement of peristaltic pumps used in the FIA by smaller, individually controlled solenoid micro-pumps makes a reduction in the size and weight of the flow system possible. Solenoid micro-pumps provides the means to reduce the power supply to 12 V and can be supplied by batteries.

However, to achieve a truly portable automated and miniaturized analytical system, a low-size, low-weight and low-power consumption detection system is necessary. In this sense, studies with photometric detectors based on light emitting diodes (LEDs) are very promising. LEDs provide low-cost, sufficiently stable and nearly monochromatic light source with high intensity. LEDs are considered to be useful in reducing the complexity of photometric devices because of absence of conventional optics. They provide simple systems for determination of specific analytes that absorb or are excited at the wavelength characteristic for the selected LEDs. Recent developments and perspectives of application of LEDs in the MPFS are described in an excellent review of Morales-Rubio et al. [5].

In many typical applications, LEDs have been used as a light source. They are combined with a proper light detector, usually a photodiode or phototransistor. These kinds of devices have been used mainly for absorbance [8–12] or fluorescence [9]

Abbreviations: DID, direct-injection detector; MPFS, multi-pumping flow system; LED, light-emitting diode; PEDD, paired emitter-detector diode.

* Corresponding author. Tel.: +48 895234410/895234801; fax: +48 895234801.

E-mail address: stankor@uwm.edu.pl (S. Koronkiewicz).

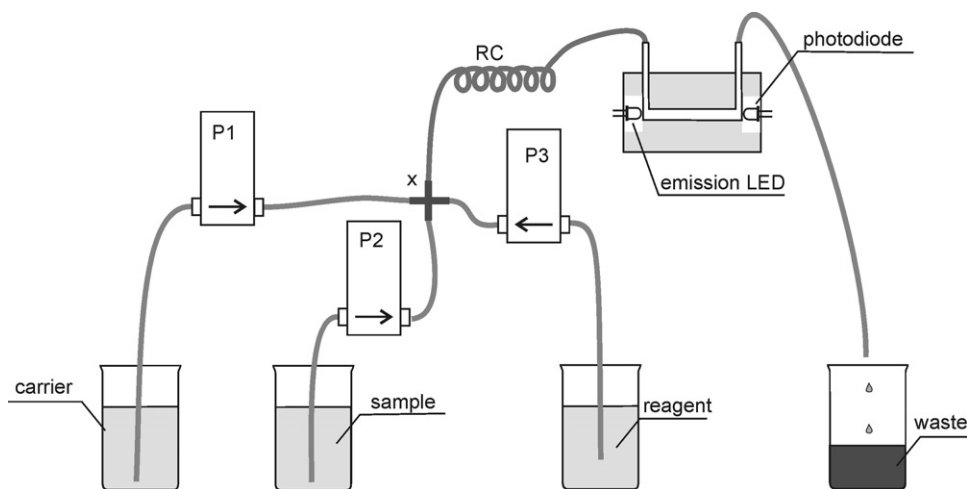


Fig. 1. A typical configuration of a multi-pumping flow system with the LED-photometry detection. P1, P2, P3 – pulse micro-pumps; X – confluence point; RC – reaction coil.

measurements. When applying to the MPFS flow manifold, LED-photodiode configuration can be used for, e.g. photometric environmental determination of iron(III), nitrite, phenol and carbaryl [10], selenium in natural water [13], speciation of chromium [12] and turbidity [14]. A typical manifold used in the MPFS flow procedure utilising LED-photodiode detection is shown in Fig. 1.

It is known that the internal photoelectric effect allows for LEDs to be used not only as light emitters, but also as light detectors. In this configuration, two identical LEDs were used [15–18]. Other configurations presented in published papers [19,20] are based on application of two properly chosen different LEDs. Recently, the utility of paired emission-detection diodes (PEDD) has become increasingly popular in flow analysis [15,19,21–23], but only a few of those PEDD applications concern the multi-pumping flow systems [21,23].

In our previous publication [23], we have proposed and described a novel photometric PEDD-detector integrated with the MPFS system. The main novelty presented there was the strategy of injection of the sample and reagent directly to the detection chamber by properly chosen pulse micro-pumps. Unlike in the typical systems (Fig. 1), the additional reaction coil was not necessary. The results obtained included a more compact and simpler flow manifold, shorter time of analysis and lower reagent consumption. In this work, an improved version of this direct-injection detector (DID) integrated with the MPFS system is proposed for the determination of Fe(III) in groundwater. Iron(III) was chosen as a model analyte because it is an important parameter in the environmental analysis. Furthermore, the chemistry of the Fe–SCN colored complexes is well-known and methods of Fe(III) determination are described in many publications, some of which also concerning the MPFS systems equipped with a classical spectrophotometer [7,24] or an LED-photodiode detection system [10]. The analytical parameters of the method presented are described and evaluated in this work.

2. Materials and methods

2.1. Reagents and solutions

Potassium thiocyanate, hydrochloric acid and hydrogen peroxide were obtained from POCh (Gliwice, Poland). A 100 mg L⁻¹ stock standard solution of Fe(III) was prepared by dilution of AAS standard (WZORMAT, Poland). Working standard solutions were prepared by appropriate dilution of stock solution with water and HCl to obtain the final concentration of Fe(III) ions from 0.5 to

15 mg L⁻¹ and H⁺ ions of 0.5 mol L⁻¹ in every solutions. A 20% (w/v) stock solution of KSCN (POCh, Poland), used as a chromogenic reagent, was prepared by appropriate dissolving of crystalline KSCN in water. Working solutions of KSCN were prepared by appropriate dilution of stock solution with water. As a carrier, a solution of HCl of concentration 0.5 mol L⁻¹ was used. The carrier also contained a detergent: sodium salt of dodecyl benzenesulfonic acid (Fluka, Buchs, Switzerland).

Samples of groundwater were obtained from the wells situated in Bukwald 63, 60 and 59, district Olsztyn, Poland. Sample no.1 originated from drilled well, 70 m deep. Samples were acidified with hydrochloric acid directly after collection [25]. Hydrogen peroxide (POCh, Poland) was chosen as an oxidising reagent to convert iron(II) to iron(III). A certified reference sample of groundwater ERM®-CA615 (IRMM – Institute for Reference Materials and Measurements) was used for evaluation of accuracy of the proposed method.

All solutions were prepared with analytical-grade chemicals and with deionised water obtained from a Milli-Q (Millipore) water purification system (resistivity > 18.2 MΩ cm).

2.2. Pumps, LEDs and software

The solenoid-operated pulse-micropumps were purchased from Bio-chemValve Inc. (Boonton, USA) and have an internal volume of 10 μL (product no. 120SP1210-4TE) or 20 μL (product no. 120SP1220-4EE). The flow lines were made of a PTFE tube (ID 0.8 mm) obtained from Bio-chemValve (product no. 008T16-080-20).

The maximum of the emission spectrum of the LED used in the integrated PEDD as a light source matched the maximum of absorption of the Fe(III)–SCN complex ($\lambda_{\max} = 470$ nm [25]). As an emission diode, a blue LED (Kingbright L-7113PBC-A, $\lambda_{\max} = 470$ nm) was chosen. As a detection diode – a green LED with emission $\lambda_{\max} = 520$ nm was selected, since it was best suited for detection of light emitted by the blue diode [20]. The LEDs were purchased in a local electronics parts shop.

The PEDD detector and pulse-micropumps were PC-controlled by the measurement system of our construction [26]. The software was developed in Delphi programming language and enables the user to select the LED voltage or current and to record photocurrent or photopotential of an LED. Another task of this system was to control the work of the solenoid micro-pumps and to calibrate the signal of absorbance.

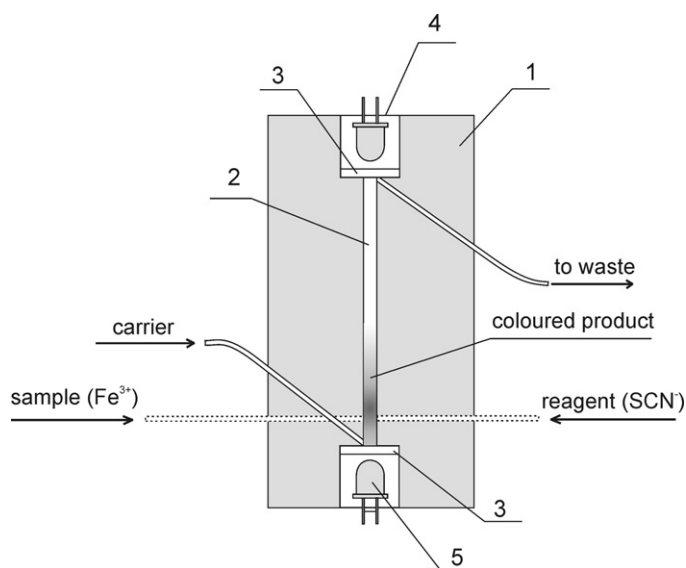


Fig. 2. Diagram of the DID-PEDD detector dedicated for Fe(III) determination. 1 – body of the detector; 2 – reaction-detection chamber; 3 – transparent glass windows; 4 and 5 – emission and detection LEDs.

2.3. Direct-injection detector

Direct-injection detector (DID) was made from one block of Teflon (Fig. 2) and was similar to the one previously described [23]. Inside this block there is a tube-shaped reaction chamber of 20 mm in length and 2 mm in diameter (the total volume of about 60 μL). The reaction chamber also acts as a photometric detection channel. We used two paired LEDs situated at the opposite ends of the reaction-detection chamber. Both of those LEDs were separated from the chamber interior with transparent glass windows. The windows were made of normal optical glass. The inlets of the sample and reagent were situated perpendicularly to the axis of reaction-detection chamber. Additionally, these inlets were placed opposite each other. Such a location promotes effective mixing conditions.

It is recommended for the volume of the reaction-detection chamber to be larger than the total volume of the sample (solution containing Fe(III) ions) and reagent (solution of SCN^- ions). That way, the entire volume of the injected solution involved in the creation of coloured product remains inside the detector, on the optical pathway. For this reason, the nominal volume of the micro-pumps used and number of strokes should be suitable, matched to the volume of reaction-detection chamber. In order to effectively and swiftly clean the chamber with the carrier, it is advisable to use a pump of nominal volume of, e.g. 20 or 50 μL .

The prototype of the DID detector described previously [23] was sensitive to air bubbles, which have tendency to appear on the optical pathway. To avoid this problem, first of all we changed the alignment of the carrier inlet and waste outlet. Setting them at an acute angle, not perpendicularly to the axis of reaction-detection chamber, prevents the bubbles from remaining within that chamber. Teflon is known as a strongly hydrophobic material and unfortunately, despite the change in the detector construction, we still had occasional problems with air bubbles. To avoid adhesion of the air bubbles to the poorly wettable walls of the detector, addition of high-grade detergent, the sodium salt of dodecyl benzenesulfonic acid, to carrier was applied.

To use LEDs in this direct-injection detector, they were first placed in special holders. Both holders were prepared as a screw of a diameter adopted to the diameter of the holes made before in the body of the detector. Using the drill bit fitted to the diameter of

the LEDs (5 mm), a hole was drilled through the screw. Then, both of the LEDs were placed inside the holders and if necessary stuck to them with thermal glue.

2.4. Flow manifold and procedures

The flow system was designed to employ three solenoid micro-pumps. The pumps were responsible for insertion of the solution, control of the inserted volume, time and sequence of insertion, transport into and out of the reaction-detection chamber. The schematic diagram of the flow network used is shown in Fig. 3. The solutions were injected directly into the detector chamber.

Experiments were carried out with diaphragm micro-pumps operated by a solenoid. The pumps were switched ON/OFF by a programmed sequence of electric pulses. When the solenoid coil of the pump was energized (ON), the diaphragm was pulled back causing the insertion of a solution into the micro-pump chamber through the input channel. When the applied voltage was turned OFF, the solenoid was de-energized and the spring forced the diaphragm back into the stable position. As a result, the solution was dispensed through the micro-pump output channel. The solenoid micro-pumps were operated independently and individually. They provide precise and synchronized injection of sample, reagent and carrier solutions. An example of the program applied to control the work of solenoid pumps is shown below:

V1 = 3, 0.2, 0.2, 0.2
V2 = 3, 0.2, 0.2, 0.2
V3 = 23, 9*(0.5, 0.5), 0.5

During the first 3 s – the signal of absorbance was recorded for the base line. Next, during the time of 0.2 s, the voltage impulse was applied (ON) to the pump 1 (Fig. 3) and the sample (Fe^{3+} solution) was aspirated into the interior of the pump. Then, after the voltage dropped (OFF), during the next 0.2 s, the sample solution was pressed out of the pump into the reaction-detection chamber. Then, during the next 0.2 s, the sample was aspirated and injected into the chamber again (ON). As a result, we used double, subsequent injection. At the end, the pump was switched OFF again and remained deactivated for the rest of the cycle duration.

The program of the pump 2 was identical to the first. Therefore, two solutions: Fe^{3+} and SCN^- were simultaneously injected into the reaction-detection chamber from opposite directions, in countercurrent.

Pump 3 was inactive for the first 23 s. Then it was employed to wash the analytical path using a carrier solution. To ensure the reaction-detection chamber was clean and ready for the next measuring cycle, pump 3 repeated the sequence of switching ON and OFF 10 times. As a result, the total volume of 200 μL was pumped through the chamber.

3. Results and discussion

3.1. Optimization of concentration of thiocyanate

A thiocyanate solution in an appropriate concentration was used as a chromogenic reagent. The formation of colored Fe(III)-thiocyanate complexes is used for a long time for the spectrophotometric determination both Fe(III) [7,10,24,27,28] and thiocyanate [29]. Thiocyanate ions react with iron(III) to form a series of complexes: $[\text{Fe}(\text{SCN})_n]^{+3-n}$ where $n = 1-6$. The concentration of thiocyanate determines the number of thiocyanate ions that are coordinated around each iron(III) ion. At a relatively low thiocyanate concentration, the form $\text{Fe}(\text{SCN})^{2+}$ predominates. This form

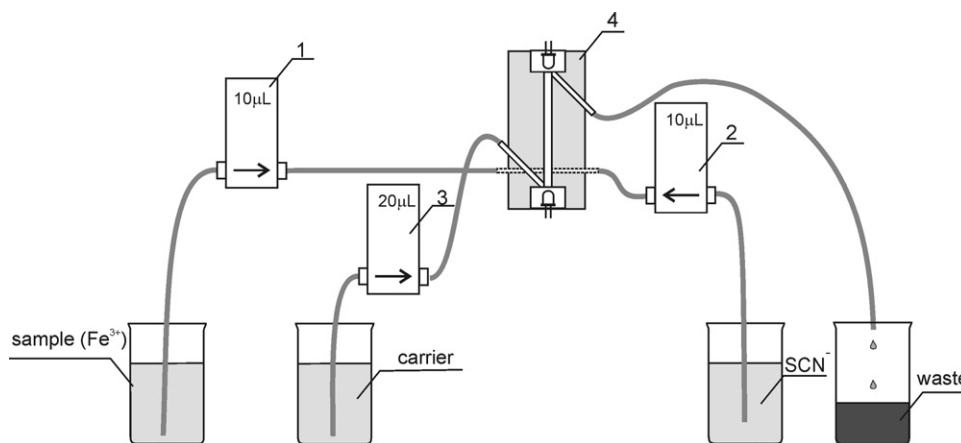


Fig. 3. Flow manifold used for Fe(III) determination. 1, 2, 3 – solenoid pulse micro-pumps; 4 – direct-injection detector.

is responsible for the characteristic reddish-brown colour of the complex.

The influence of the concentration of thiocyanate ions on the analytical signal was examined in the range from 2.5 to 20% (w/v). The concentration was optimized by studying its effect on both: the level of analytical signal and the baseline. As can be seen in Fig. 4 the analytical signal increased with the increasing of KSCN concentration. Above the concentration of 5% we also observed an increase in the baseline level. Therefore, the concentration of 5% (w/v) of KSCN was chosen for subsequent studies.

3.2. Optimization of the sample volume

Working with the MPFS system, we utilized the fact that the sample/reagent injection strategy affected not only solution transport but also reaction zone homogenization but also the magnitude of the analytical signal [2–4]. According to the Lambert–Beer law, the absorbance depends on the number of molecules which are able to absorb the light. When using the direct-injection detector, it is advisable to adjust the total volume of injected solutions, i.e. sample and reagent, to the volume of the reaction-detection chamber [23]. The volume of the chamber was 60 µL. We checked the influence of the sample volume on the absorbance signal in the range from 10 to 40 µL. To promote effective mixing conditions, we applied the same volume of the reagent. Obtained results are presented in Fig. 5. The absorbance increased noticeably with the increase in the sample volume. However, for samples of larger volume, 30 µL and 40 µL, we observed a lower repeatability of the signal. When the total volume of the sample and reagent equaled or exceeded the volume of the reaction-detection chamber, the probability that

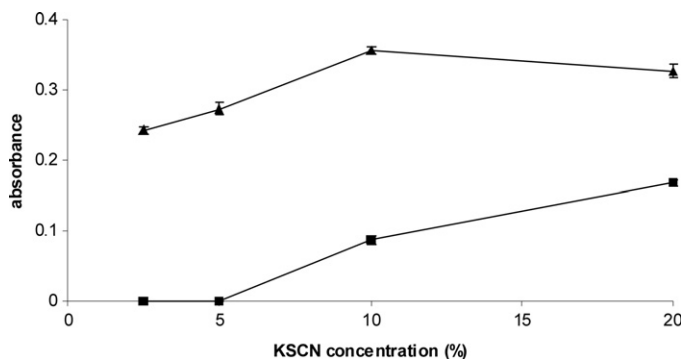


Fig. 4. Influence of the thiocyanate concentration on the analytical signal (▲) and the baseline (■). Each point represents the mean of at least four consecutive measurements, bars indicate the standard deviations.

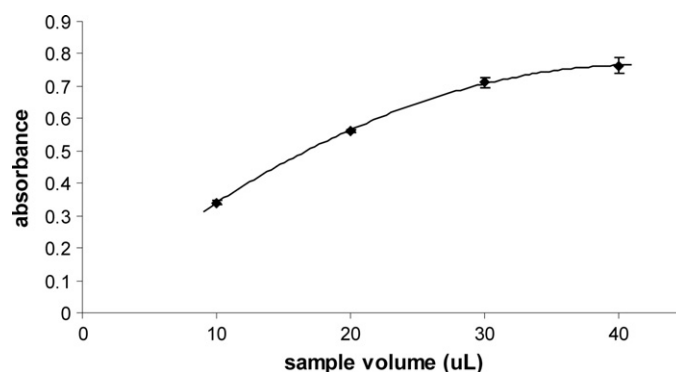


Fig. 5. The effect of the sample volume on the analytical signal. Fe(III) concentration 5 mg L⁻¹. Each point represents an average of five consecutive measurements, bars indicate the standard deviation of the obtained value.

some absorbing light molecules can escape out of the detection chamber increased. To obtain high and repeatable analytical signal the sample volume of 20 µL is recommended.

3.3. Influence of Fe(III) concentration on the changes in the analytical signal.

The application of the direct-injection detector allows for the colour development to be monitored. Our studies indicate that the kinetics of the absorbance changes and the shape of the analytical signal depend on the iron(III) concentration (Fig. 6). The

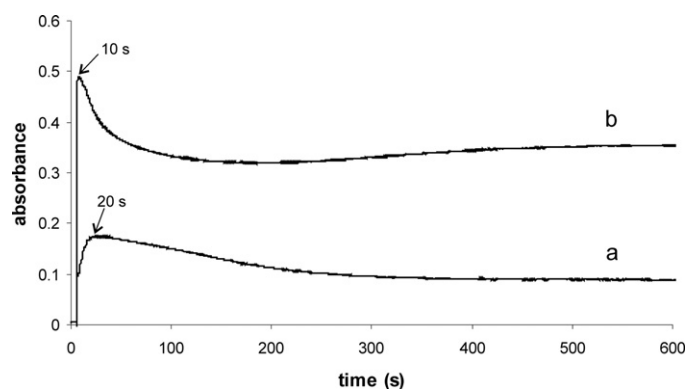


Fig. 6. Influence of the sample concentration on the changes in analytical signal with the time. Fe(III) concentration: (a) 2 mg L⁻¹, (b) 10 mg L⁻¹; sample volume: 10 µL, single injection; stop flow: 595 s. The time required to obtain the maximum of absorbance is indicated.

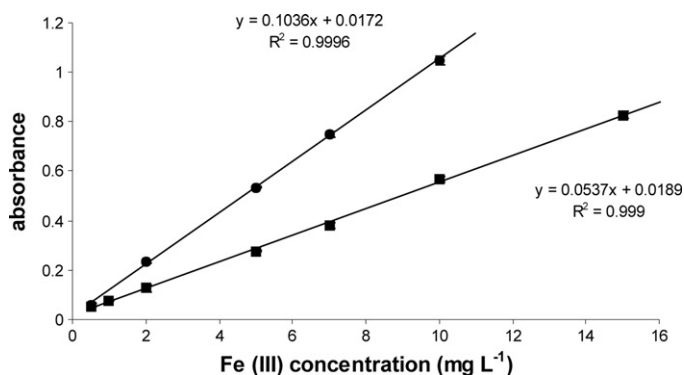


Fig. 7. The calibration graphs for iron(III) obtained for different sample volumes: (a) 10 μL , single injection; (b) 20 μL , double injection; stop flow: 20 s. Each point represents an average of at least five consecutive measurements.

time necessary to obtain the maximum of absorbance depended on the concentration of iron(III). When the Fe(III) concentration was relatively low, in the range about 1–5 mg L^{-1} , the maximum of absorbance was achieved at about 20 s into a measurement cycle. Using standard Fe(III) solution of about 10 mg L^{-1} or higher we observed a fast increase in the absorbance signal, followed by a relatively fast decrease. As a result, the maximum of the absorbance was observed in a relatively short time of 10 s.

The colour of the Fe(III)–SCN complex is unstable. It was noticed [25] that the intensity of the colour decreases by up to several percent after 30 min and up to 50% of its initial value after 6 h. This was explained by the reduction action of thiocyanate on the iron(III). Therefore, an analytical signal should be measured after a fixed amount of time – the same for the sample and standards, usually optimized, which is easy achievable in flow conditions [29].

When preparing the calibration graph, it is possible to take into account the absorbance measured at a fixed time, e.g. after 10 or 20 s or at the maximum of the absorbance signal. We obtained the following calibration graph equations:

1. $A = 0.1225[\text{Fe}^{3+}] + 0.0292$ ($R^2 = 0.998$) – the absorbance was measured 10 s after injection of standard and thiocyanate.
2. $A = 0.1116[\text{Fe}^{3+}] + 0.0695$ ($R^2 = 0.999$) – the absorbance was measured 20 s after injection of standard and thiocyanate.
3. $A = 0.1186[\text{Fe}^{3+}] + 0.0649$ ($R^2 = 0.9962$) – the absorbance was read at the maximum of the analytical signal.

The calibration graphs did not differ significantly and for quantitative analysis every strategy seems to be appropriate. Although, from the point of view of the best throughput, the time of the determination should be as short as possible. Therefore, the time of stop flow of 10 s seems to be favourable. The total time of the determination should be longer, because the signal of the baseline should be registered and the reaction-detection chamber needs to be washed after the analysis. Depending on the pump applied to wash the chamber, this additional time can be shortened to about 5–10 s.

Therefore, the shortest real time of the determination seems to be about 20 s and the throughput of the proposed method is about 180 determinations per hour.

3.4. Analytical parameters

The parameters of calibration graph for iron(III) depend on the volume of the sample used (Fig. 7). An increase in sample volume results in a rise in quantity of molecules which are able to absorb the light. As a result, it is possible to improve the sensitivity of the method. Increasing the sample volume from 10 to 20 μL caused an about twofold increase in the slope of calibration graph.

Simultaneously, we observed a change in the range of calibration graph. When a single injection of sample and reagent (sample volume 10 μL) was applied, the calibration graph covered the range from 0.3 to 15 mg L^{-1} . When using a double injection (sample volume 20 μL), the range was from 0.15 to 10 mg L^{-1} . Therefore, the range of calibration graph can be easily adjusted, if necessary, to the concentration of the analyte in the sample. A noteworthy fact is that the range of the calibration graph can be changed and controlled through the changes in the program of the micro-pumps, without any changes in the equipment itself. On the other hand, there is some compromise between the magnitude of the analytical signal and the cost of analysis.

The detection limit (DL), calculated as $3s_b/S$, where s_b is the standard deviation for 10 measurements of the blank and S is the slope of calibration graph, was 0.3 mg L^{-1} for a single sample and reagent injection and decreased to 0.15 mg L^{-1} for a double injection. The repeatability (R.S.D.) calculated for 10 successive injections of the standard solution 5 mg L^{-1} was 1.5%. An injection throughput of 180 injections per hour has been achieved.

The method is characterized by a very low consumption of the sample and reagent, which is only 20 μL (or even 10 μL) for each of these solutions and by a very low waste volume generation – only 0.24 mL per analysis.

3.5. Application to the real samples

The accuracy of the proposed method was evaluated in the determination of iron in Certified Reference Material (CRM) of groundwater (ERM[®]-CA615). The comparison of measured results on a certified reference material with the certified value was conducted according to the Application Note [30]. The method compares the difference between the certified and measured values with its uncertainty. After the measurement of the CRM, the absolute difference between the mean measured value (c_m) and the certified value (c_{CRM}) was calculated as:

$$\Delta_m = |c_m - c_{CRM}| = |4.85 - 5.11| \text{ mg L}^{-1} = 0.26 \text{ mg L}^{-1}$$

The uncertainty of Δ_m is u_{Δ} , that was calculated from the uncertainty of the measurement result (u_m) and the uncertainty of the certified value (u_{CRM}). As a u_m , the standard deviation of the mean measured value was used. The uncertainty u_{Δ} was calculated according to:

$$u_{\Delta} = \sqrt{u_m^2 + u_{CRM}^2} = \sqrt{0.04^2 + 0.13^2} = 0.136$$

The expanded uncertainty U_{Δ} , corresponding to a confidence level of approximately 95%, was obtained by multiplication of u_{Δ} by a coverage factor (k) equal 2:

$$U_{\Delta} = 2 \cdot u_{\Delta} = 0.272$$

The results show that $\Delta_m < U_{\Delta}$. There is no significant difference between the measured results and the certified value.

The method has been applied to the determination of iron in natural groundwater samples. The oxidation of Fe(II) to Fe(III) using hydrogen peroxide prior to the analysis allows the determination of total iron concentration in the samples.

Table 1 summarizes the results of total iron determinations and percentage recoveries of groundwater samples. The determined concentration of the iron in the examined groundwater samples was ranged from 0.60 ± 0.05 to $7.0 \pm 0.2 \text{ mg L}^{-1}$ (mean of four determinations \pm S.D.). The recovery was close to the 100% for the sample rich in iron (sample no. 1). For the samples characterized by a low content of iron, the recovery was lower and achieved the value of about 90%. This may indicate a problematic accuracy during determination of iron in samples with low concentration of this

Table 1
Results of the determination of total iron for groundwater samples.

No.	Determined concentration of iron (mg L ⁻¹)	Injected Fe(III) (mg L ⁻¹)	Found Fe(III) (mg L ⁻¹)	Recovery (%)
1. ^a	7.0 ± 0.2	1.00	0.99 ± 0.06	99
		2.00	2.04 ± 0.08	102
		3.00	2.97 ± 0.13	99
2. ^b	0.86 ± 0.09	1.00	1.00 ± 0.07	100
		2.00	1.76 ± 0.02	88
		3.00	2.60 ± 0.07	87
3. ^b	0.60 ± 0.05	1.00	0.98 ± 0.04	98
		2.00	1.86 ± 0.01	93
		3.00	2.77 ± 0.02	92

Results represent the average of at least four determinations ± S.D.

^a Dilution factor 4:6.

^b dilution factor 4:1.

Table 2
Comparison of the analytical features achieved by the proposed direct-injection detector integrated with the MPFS system and MPFS systems with typical configuration.

Parameter	MPFS and direct-injection PEDD detector	MPFS and LED-photodiode [10]	MPFS and spectrometer [28]
Reaction coil (cm)	Not exist	120	32
Carrier	0.5 mol L ⁻¹ HCl with detergent	H ₂ O	H ₂ O
Sample (Fe ³⁺) consumption (μL)	20	70	200
Reagent (SCN ⁻) consumption (μL)	20	70	200
Total waste (mL)	0.24	1.2	–
Calibration graph equation	$A = 0.1036[\text{Fe}^{3+}] - 0.0172$	$A = 0.126[\text{Fe}^{3+}] - 0.00$	$A = 0.0645[\text{Fe}^{3+}] - 0.003$
Regression coefficient, $R^2(n)^a$	0.9996 (5)	0.999 (6)	0.9986 (7)
Working range (mg L ⁻¹)	0.15–10	–	0.2–15
DL ^b (mg L ⁻¹)	0.15	0.2	0.2
Repeatability ^c (%)	1.5	2.3	1.0
Injection throughput (injections h ⁻¹)	180	100	120

^a Regression coefficient, number of standards in bracket.

^b Detection limit calculated as $3s_b/S$, where s_b is the standard deviation for 10 measurements of the blank and S is the slope of the calibration graph.

^c R.S.D. – relative standard deviation for 10 independent analyses of sample containing 5 mg L⁻¹.

analyte. However, the method presents a good accuracy considering the complex composition of the groundwater samples. The results obtained show that the proposed method can be applied to the determination of total iron in groundwater samples.

3.6. Comparison of DID-MPFS with other MPFS systems

The comparison of the results obtained using the proposed direct-injection photometric detector integrated with the MPFS system with those obtained from the MPFS systems but with typical configuration (Fig. 1), employed LED-photodiode flow detector [10] or a commercially available spectrophotometer with flow cell [28] was carried out. The results are summarized in Table 2.

The proposed flow system is simpler in construction because of the absence of a reaction coil. The flow lines are shorter. The volume of the solution that must be transported in the system is lower. Pumps working in the proposed configuration perform a lower number of strokes, are less loaded and, as a result, exhibit a longer lifetime.

The use of a direct-injection detector considerably decreases the sample and reagent consumption. It is possible to significantly minimize the waste generation and increase the throughput. The detection limit and repeatability of compared methods are similar.

4. Conclusions

The direct-injection photometric detector integrated with multi-pumping flow system developed in this study proved to be suitable for the determination of total iron in groundwater samples. Idea of the sample and reagent injection directly into the photometric detection chamber allows reduction in the sample and reagent

consumption. The considerable reduction in the time and cost of analysis is possible. Low-waste generation makes this method environmentally friendly. The application of LED technology allows for simpler construction of the detection system and allows the total cost of the flow system to be lowered without deterioration in the analytical parameters such as the sensitivity and working range. The system is easy to operate, compact, small in size and weight, and requires 12 V in supply voltage, which is desirable for truly portable equipment. These characteristics suggest that this equipment could be employed in mobile, Green Chemistry laboratories.

References

- [1] M. Trojanowicz (Ed.), *Advances in Flow Analysis*, Wiley-VCH, Weinheim, 2008.
- [2] R.A.S. Lapa, J.L.F.C. Lima, B.F. Reis, J.L.M. Santos, E.A.G. Zagatto, *Anal. Chim. Acta* 466 (2002) 125–132.
- [3] J.L.F.C. Lima, J.L.M. Santos, A.C.B. Dias, M.F.T. Ribeiro, E.A.G. Zagatto, *Talanta* 64 (2004) 1091–1098.
- [4] J.L.M. Santos, M.F.T. Ribeiro, A.C.B. Dias, J.L.F.C. Lima, E.E.A. Zagatto, *Anal. Chim. Acta* 600 (2007) 21–28.
- [5] A. Morales-Rubio, B.F. Reis, M. Guardia, *Trends Anal. Chem.* 28 (2009) 903–913.
- [6] J.A.V. Prior, J.L.M. Santos, J.L.F.C. Lima, *Anal. Bioanal. Chem.* 375 (2003) 1234–1239.
- [7] C. Pons, R. Forteza, A.O.S.S. Rangel, V. Cerda, *Trends Anal. Chem.* 25 (2006) 583–588.
- [8] M. Trojanowicz, J. Szpunar-Lobinska, Z. Michalski, *Microchim. Acta I* (1991) 159–169.
- [9] P.K. Dasgupta, I.Y. Eom, K.J. Morris, J. Li, *Anal. Chim. Acta* 500 (2003) 337–364.
- [10] E. Rodenas-Torralba, F.R.P. Rocha, B.F. Reis, A. Morales-Rubio, M. Guardia, *J. Autom. Meth. Manage. Chem.* 2006 (2006) 1.
- [11] A.F. Lavorante, A. Morales-Rubio, M. Guardia, B.F. Reis, *Anal. Chim. Acta* 600 (2007) 58–65.
- [12] C.K. Pires, B.F. Reis, A. Morales-Rubio, M. de la Guardia, *Talanta* 72 (2007) 1370–1377.
- [13] R.N. Fernandes, B.F. Reis, A. Morales-Rubio, M. Guardia, *J. Braz. Chem. Soc.* 20 (2009) 1242–1248.

- [14] E. Rodenas-Torralba, A. Morales-Rubio, A.F. Lavorante, B.F. Reis, M. Guardia, *Talanta* 73 (2007) 742–747.
- [15] M.O. Toole, K.T. Lau, D. Diamond, *Talanta* 66 (2005) 1340–1344.
- [16] K.T. Lau, E. McHugh, S. Baldwin, D. Diamond, *Anal. Chim. Acta* 569 (2006) 221–226.
- [17] L. Tymecki, R. Koncki, *Anal. Chim. Acta* 639 (2009) 73–77.
- [18] E. Mieczkowska, R. Koncki, L. Tymecki, *Anal. Bioanal. Chem.* 399 (2011) 3293–3297.
- [19] M. O'Toole, K.T. Lau, R. Shepard, C. Slater, D. Diamond, *Anal. Chim. Acta* 597 (2007) 290–294.
- [20] M. O'Toole, K.T. Lau, B. Shazmann, R. Shepherd, P.V. Nesterenko, B. Paull, D. Diamond, *Analyst* 131 (2006) 938–943.
- [21] L. Tymecki, K. Strzelak, R. Koncki, *Talanta* 79 (2009) 205–210.
- [22] M. Pokrzywnicka, D.J. Cocovi-Solberg, M. Miro, V. Cerda, R. Koncki, L. Tymecki, *Anal. Bioanal. Chem.* 399 (2011) 1381–1387.
- [23] S. Kalinowski, S. Koronkiewicz, *Talanta* 86 (2011) 436–441.
- [24] C. Pons, R. Forteza, V. Cerda, *Anal. Chim. Acta* 528 (2005) 197–203.
- [25] Z. Marczenko, *Spectrophotometric Determination of Elements*, Ellis Horwood, Chichester, 1976.
- [26] <http://pracownicy.uwm.edu.pl/kalinow>.
- [27] K. Oguma, O. Yoshioka, *Talanta* 58 (2002) 1077–1087.
- [28] C. Pons, R. Forteza, V. Cerda, *Anal. Chim. Acta* 550 (2005) 33–39.
- [29] J.F. van Staden, A. Botha, *Anal. Chim. Acta* 403 (2000) 279–286.
- [30] http://www.erm-crm.org/ERM_products/application_notes/application_note.1.